# *ATOMIZATION AND POWDER PROCESSING OF HIGH TEMPERATURE FERRITIC STAINLESS STEEL*

***I.E. Anderson[1], J. R. Rieken[2] , M.J. Kramer[1], and D. Byrd[1]***

***[1]Division of Materials Sciences and Engineering, Ames Laboratory (USDOE), Ames, IA***

***[2]Material Science and Engineering, Iowa State University, Ames, IA***

Presented at: **24TH ANNUAL CONFERENCE ON FOSSIL ENERGY MATERIALS**

Pittsburgh, Pennsylvania

May 25, 2010

*Support from the Department of Energy-Office of Fossil Energy is gratefully acknowledged through Ames Laboratory contract no. DE-AC02-07CH11358*

X100 100µm

THE Ames Laboratory
Creating Materials & Energy Solutions
U.S. DEPARTMENT OF ENERGY

U.S. DEPARTMENT OF ENERGY

# *Future Generation Coal-Fired Power Plant Needs*

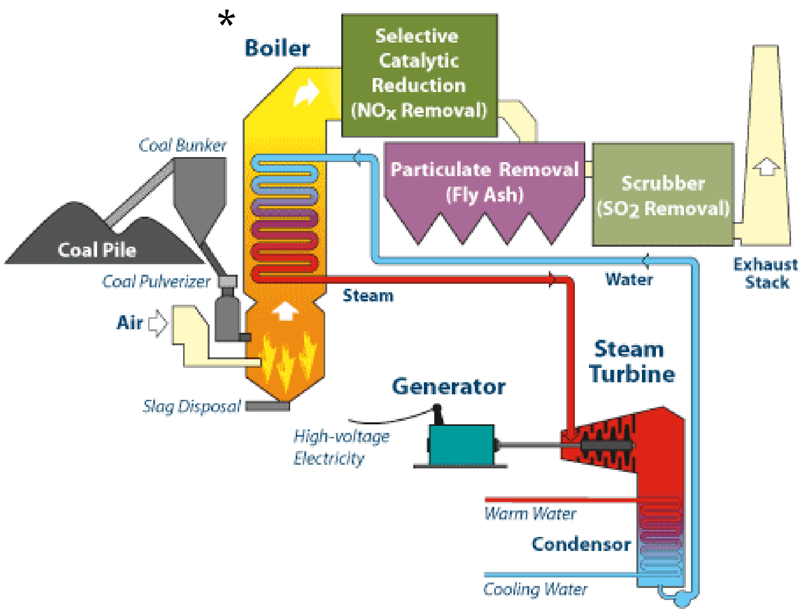


## A-USC Steam Coal Fired Power Plants:

- **Boiler materials**
- **Heat exchanger tubing**
- **Exhaust liner**
- ***760°C at 35MPa with Supercritical Steam***

*R. Viswanathana, et al., J. Press. Ves. and Pip., 2006. **83**: p. 778-783.

## Material Choices

| Material | Cost/kg (USD) | Notes |
|---|---|---|
| Ferritic Stainless Steel | ~$2-5 | 446 Plate form |
| Austenitic Stainless Steel | ~$3-7 | 316L Plate form |
| F/M Fe-9Cr steels | ≤$5.50 | Plate form |
| Ni-based | ~$30-35 | Inconel 718 Sheet (Special Metals)<br>Inconel 617 (Special Metals) |
| Fe-based ODS | ~$165<br>~$345 | MA956 Sheet (Special Metals)<br>PM 2000 (Plansee) |
| V-4Cr-4Ti | ~$200 | Plate form (Average between 1994 and 1996 US fusion program large heats) |
| $SiC_f/SiC_m$ composites | ~$1000<br>~$200 | Chemical vapor infiltration, and<br>Chemical vapor reaction |

ODS Processing Cost!!

J.T. Busby, J. Nuc. Mat., 2009. **392**: p. 304

K. Savolainen, J. Mononen, R. Ilola, and H. Hänninen, 2005, Helsinki University of Technology, Laboratory of Engineering Materials Publications.

S.J. Zinkle and N.M Ghoniem, Fusion Engineering and Design 2000. **51**(52): p. 55-71.

# Motivation

**Mechanical Alloying:**

- A high-energy mixing process that violently blends master alloy powders with nano-metric oxide powders into a supersaturated solid solution, during which complex folding, cold welding, and fracturing of the powders takes place in a high-energy mill
- **MA processing* can take numerous hours of milling time (t>40hr), which can lead to high levels of contamination from milling debris and gas environment**
- Hot deformation consolidation and recrystallization can lead to an anisotropic microstructure and directional mechanical properties

***This complex process can lead to an extremely high raw material cost, e.g., ~$340/kg for PM2000.**

*J.T. Busby, J. Nuc. Mat., 2009. **392**: p. 304

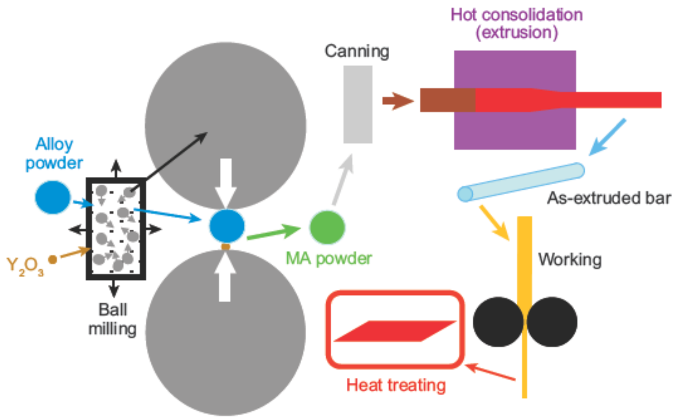


G.R. Odette, et al., Annu. Rev. Mater. Res., 2008. **38**: p. 471-503

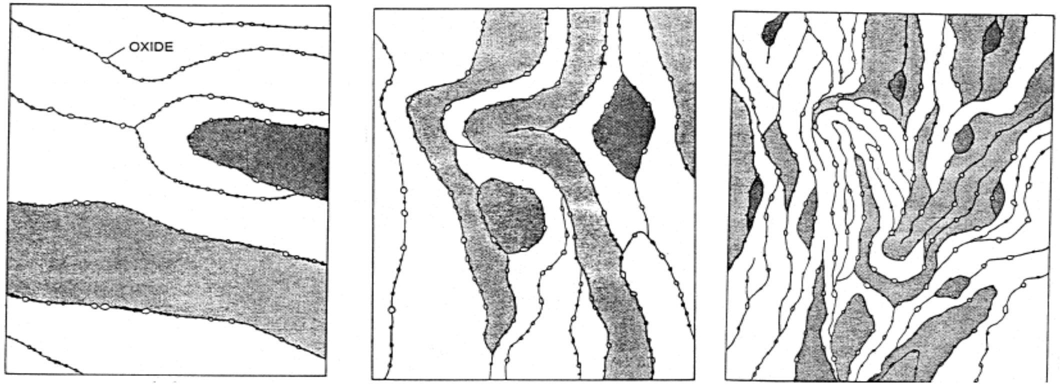


C. Suryanarayana, Prog. in Mat. Sci., 2001. **46**: p. 1-184

# *Processing Comparison*

* **Mechanical Alloying**

- Long milling times
- Batch commercial process (~200 kg)
- Powder contamination (carbon and milling debris)
- Anisotropic microstructure

** **Gas Atomization (RSP)**

- Higher processing rates (10-100 kg/min)
- Continuous processing capacity
- Minimized contamination
- Isotropic microstructure

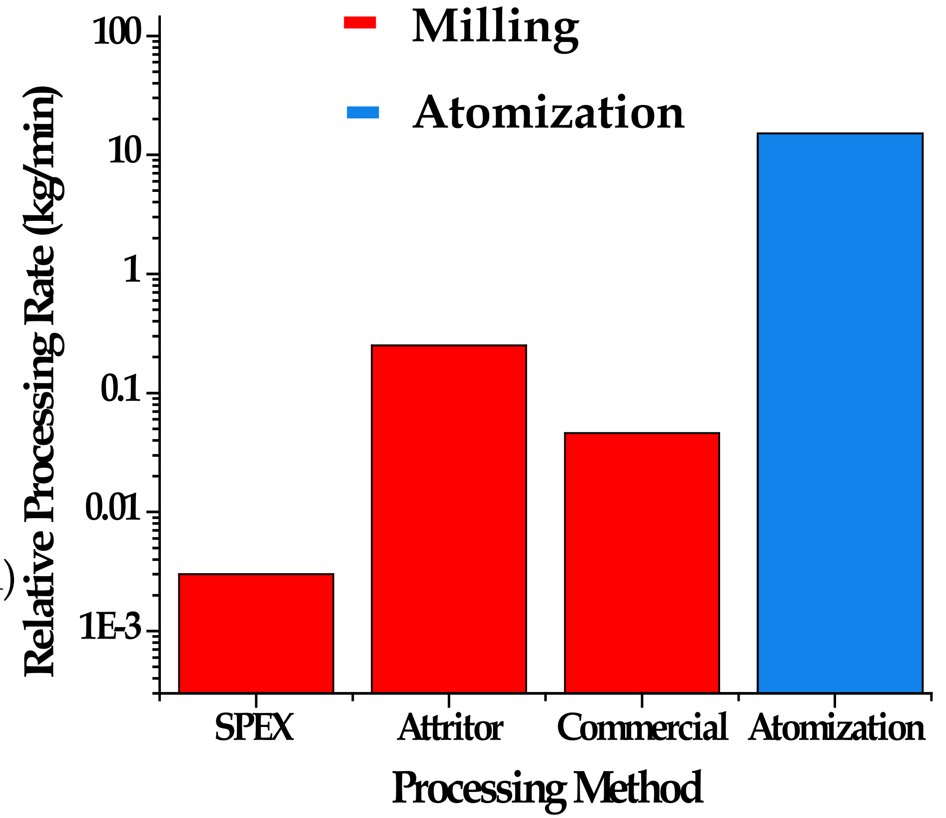


Increased powder processing rates, using gas atomization, could promote a significant reduction in raw material cost (~3-5X)

*C. Suryanarayana, ASM Handbook, Vo. 7, ASM International, Materials Park, OH, 1998, pp. 80-90.

**R.M. German, *Powder Metallurgy and Particulate Materials Processing*, 2005, MPIF, Princeton, NJ.

# New Simplified Gas Atomization Process

1) Gas Atomization Reaction Synthesis (GARS)* – *in situ* alloying
   - Oxide dispersion forming precursor powder
2) Hot Isostatically Pressed to Full Consolidation
   - Dispersoid phase formation
   - Equiaxed grain structure and isotropic mechanical properties
3) Thermal and Mechanical Treatment
   - Dislocation substructure formation (ultimate strengthening)

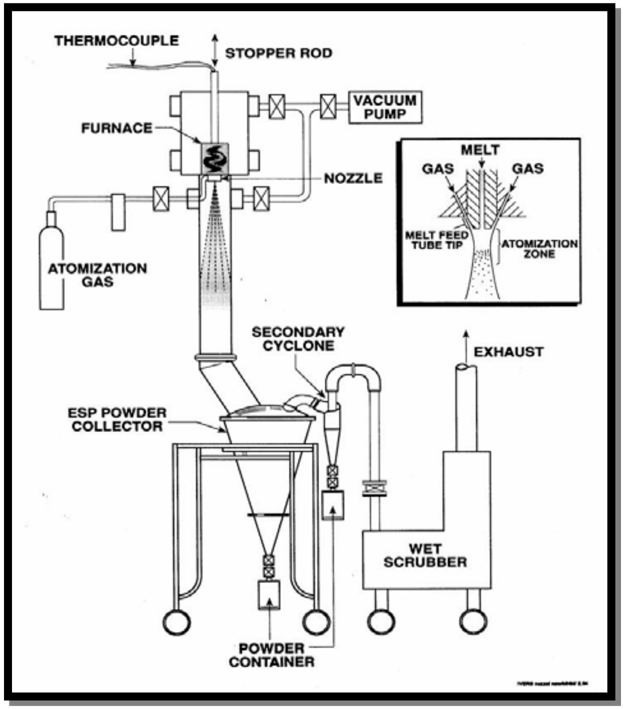


**Eliminates inefficient mechanical alloying and minimizes directional deformation processing**

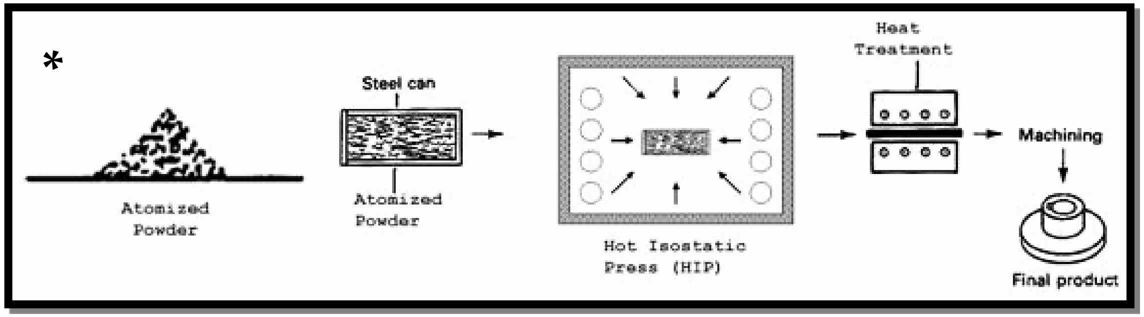


* R.L. Terpstra, et al., Advances in Powder Metallurgy and Particulate Materials, 2006.



*I.E. Anderson, et al., *Gas atomization synthesis of refractory or intermetallic compounds and supersaturated solid solutions*, USPTO no. 5,368,657. 1994.

# Chemical Reservoir – Alloy Design

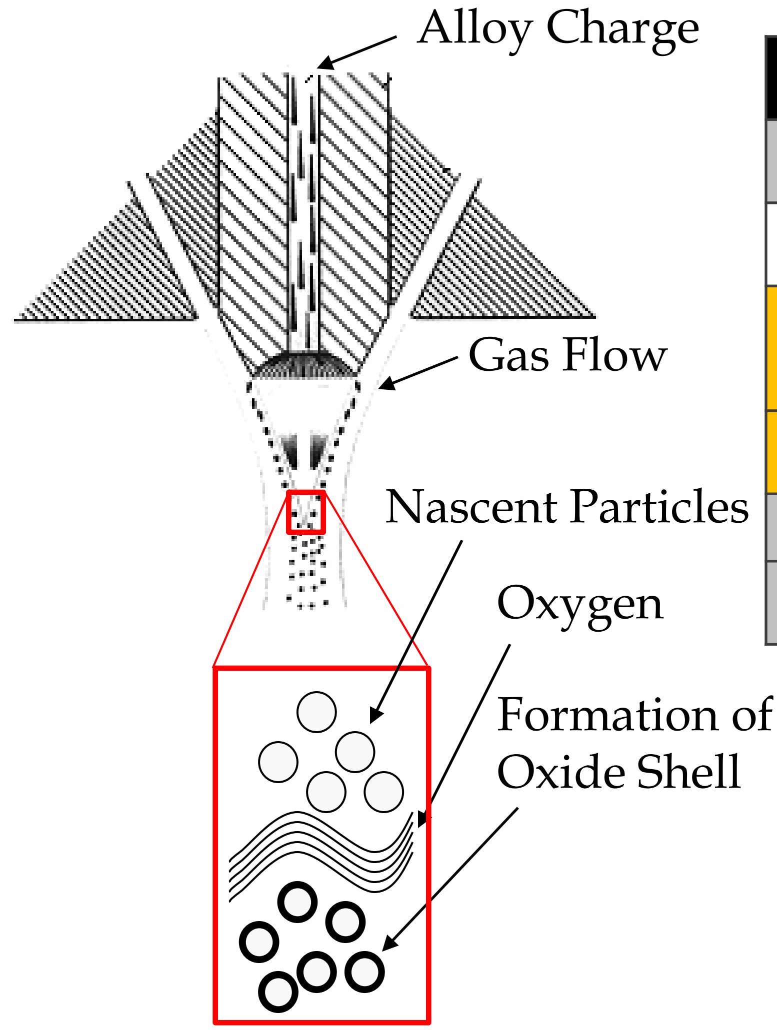


| Element | Alloying Motivation | Approx. Conc. (at.%) |
|---|---|---|
| **Chromium** | Surface reactant and corrosion resistance | 15.0-16.0 |
| **Yttrium** | Highly stable nano-metric oxide dispersoid former | 0.1-0.2 |
| ***Titanium*** | Surface reactant, dispersoid stabilizer, and interstitial impurity scavenger | 0.4-0.5 |
| ***Hafnium*** | Dispersoid stabilizer and interstitial impurity scavenger | 0.2-0.3 |
| **Tungsten** | Solid solution strengthener | 1.0 |
| **Oxygen (reactive gas)** | Surface oxidant and nano-metric oxide dispersoid former | 0.35-0.70 |

**GARS Processing:**

- **Rapid Solidification Process (solute trapping)**
- **Reactive gas mixture (Ar-$O_2$)**
- **In situ surface oxidation of the most kinetically favored oxide phase (metastable Cr-enriched oxide)**

# Dispersoid Formation Theory

**Oxygen Exchange Reaction**

- Dissociation of the less stable prior particle boundary (PPB) oxide
- Oxygen diffusion away from PPBs
- Nano-metric Y-enriched oxide formation

- ***Full dissociation of PPB oxide will be necessary for ideal mechanical properties***

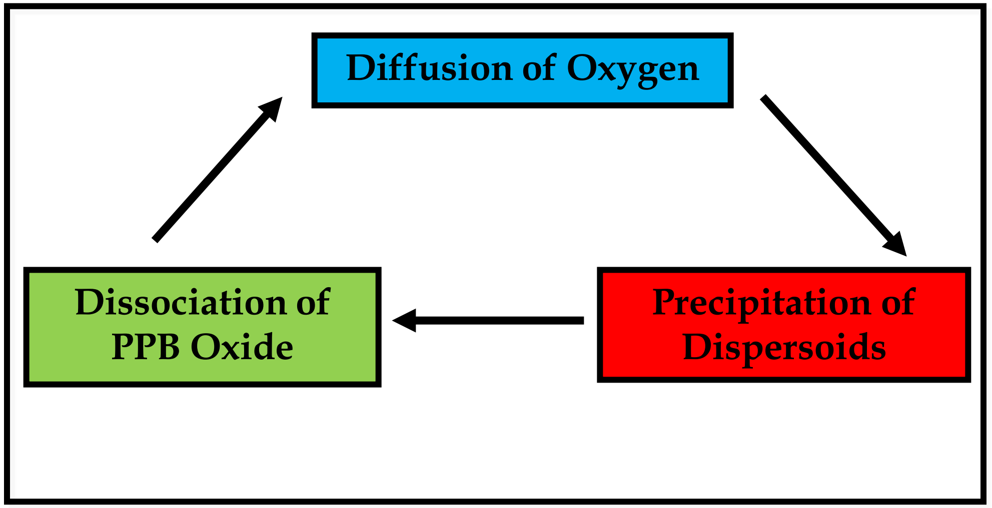


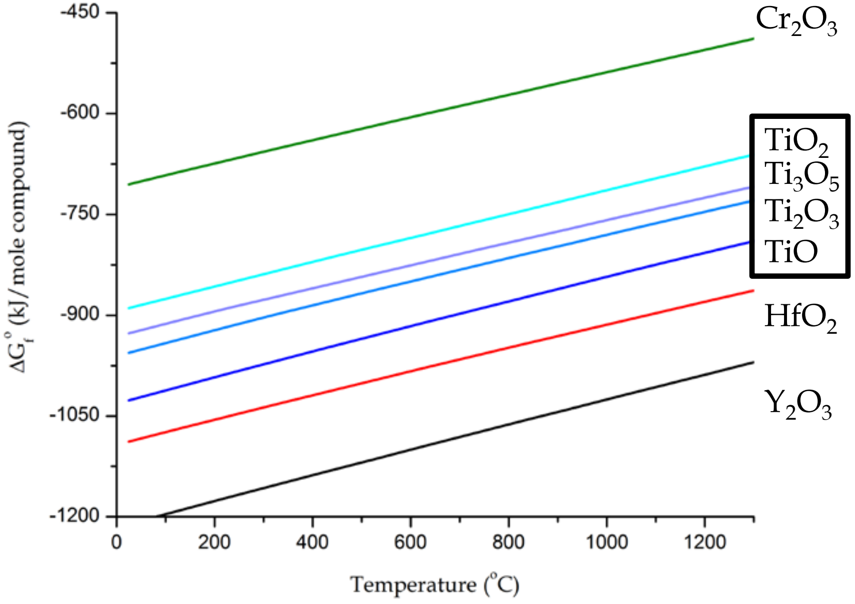


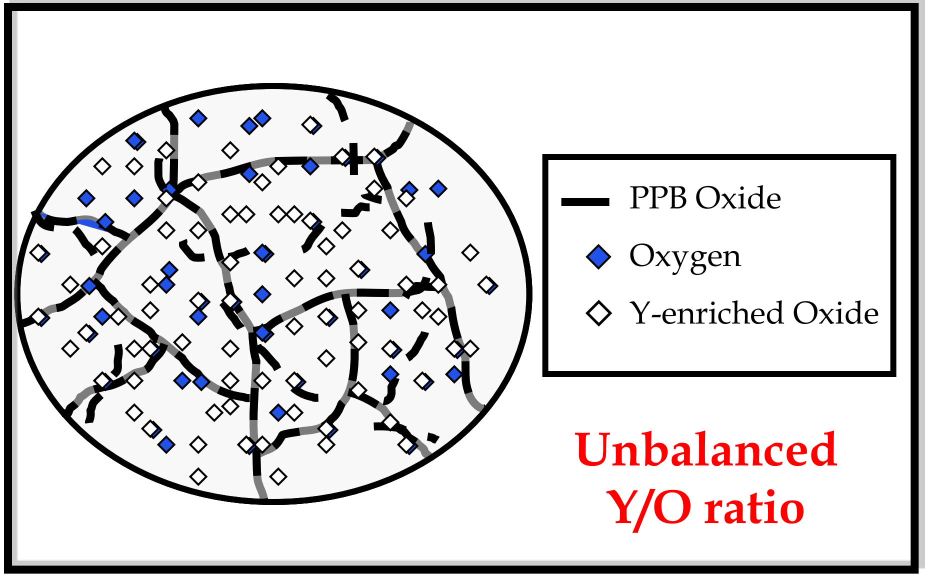




Sauert F., et al., Thermochemical Data of Pure Substances, 2nd Edition 1992.

# FY2009 Milestone Analysis

Report further results of high temperature mechanical properties of ODS alloys made from GARS processed precursor powders of Fe-Cr-X alloys. [Completion planned March 2009]

- High temperature tensile results (to 800˚C) related to fracture microstructure analysis at TMS Annual Meeting (Feb. 2009) and FEMC (May 2009).
- Improved alloy (as-consolidated) displayed tensile strength equivalent to MA956 (to 800˚C) with 3X elongation) with fully isotropic microstructure.
- Fracture analysis revealed failure linked to residual oxide phase on prior particle interfaces and confirmed need to improve oxide/solute balance in precursor powder.

Perform detailed high temperature studies of the transformation and diffusion kinetics of the consolidated ODS alloys to provide heat treatment guidance for enhanced properties. [Completion planned September 2009]

- Rhines pack measurements described high temperature oxygen diffusion and exchange reaction kinetics with intermetallic compounds at 2009 FEMC (May 2009).
- Higher oxygen diffusion rate observed than expected from diffusion modeling for high temperatures (1300˚C), i.e., oxygen diffusion is not the rate-limiting step.
- Results motivated design of lower temperature (1000-1200˚C) diffusion/internal oxidation experiments to couple with reduced temperature (700˚C) HIP consolidation.

# *Failure Analysis-Microstructure*



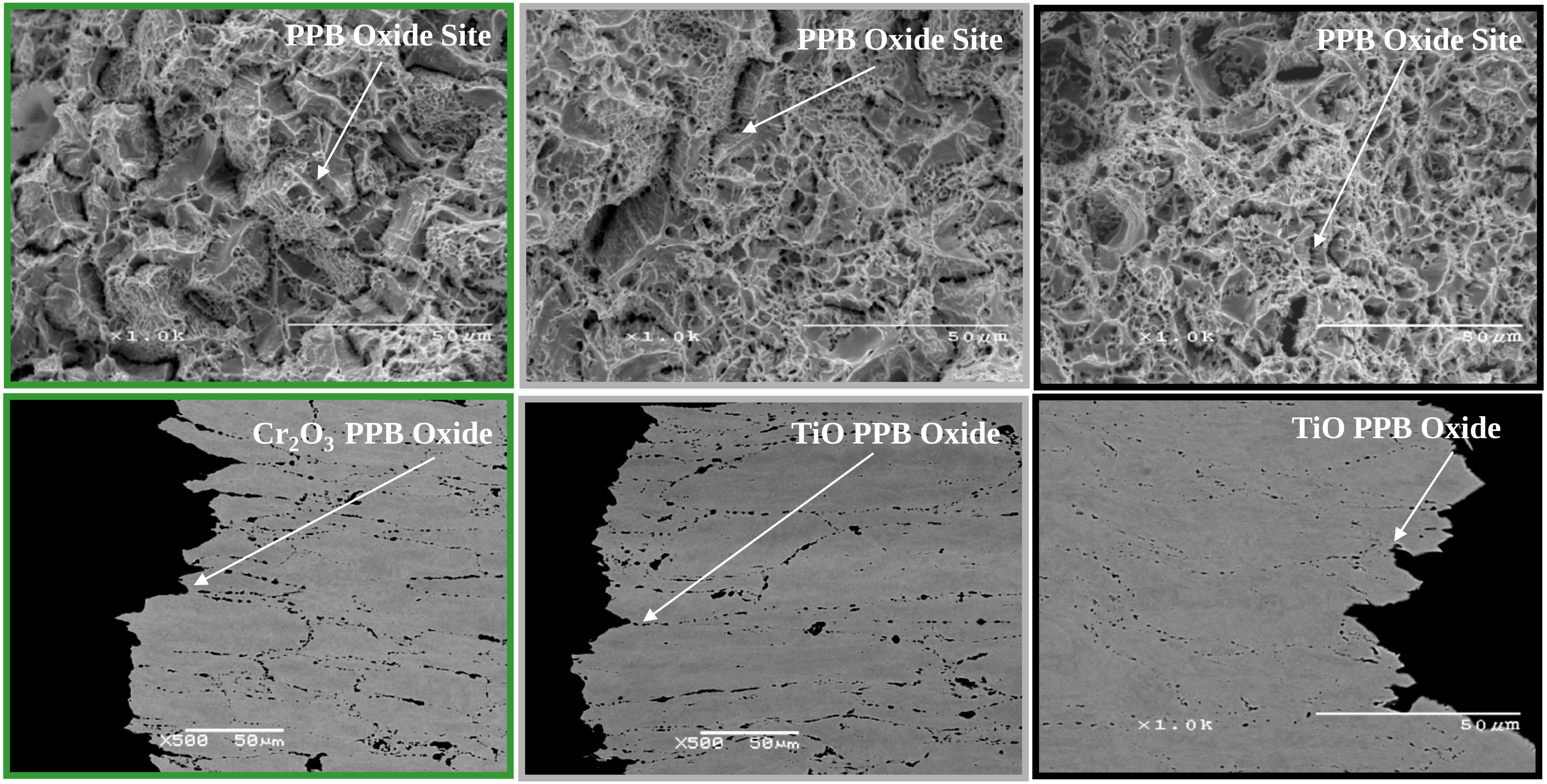


CR-112 | CR-118Ti | CR-126TiW

**Failure occurs by micro-void formation/coalescence resulting from the debonding of the matrix from residual non-ideal phases (i.e. PPB oxide)**

# *Chemical Reservoir Alloys and Experimental Parameters*

| Alloy | Fe (at.%) | Cr (at.%) | W (at.%) | Ti (at.%) | Hf (at.%) | Y (at.%) | O (at.%) | Rxn Gas (vol.%) | Rxn Gas Inlet |
|---|---|---|---|---|---|---|---|---|---|
| CR-118 | 83.47 | 15.84 | - | 0.50 | - | 0.20 | 1.67 | Ar-0.5$O_2$ | HPGA Nozzle |
| CR-144 | 82.55 | 16.16 | 0.94 | - | 0.27 | 0.08 | 0.23 | Ar-0.25$O_2$ (halo) | Über Halo |

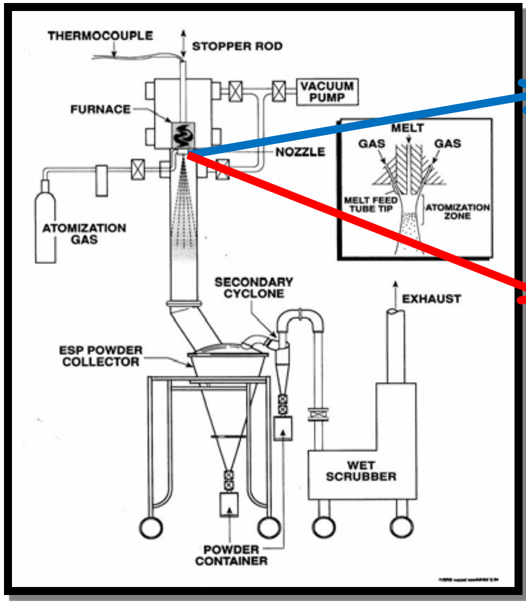


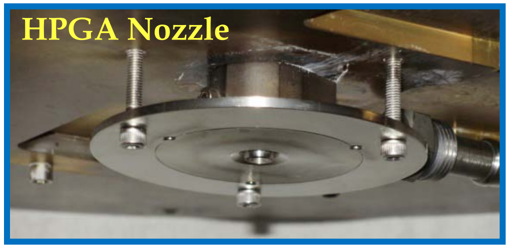



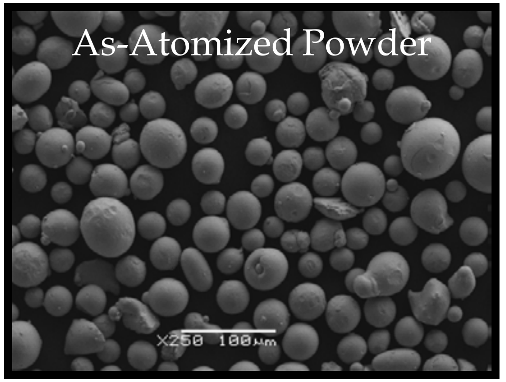


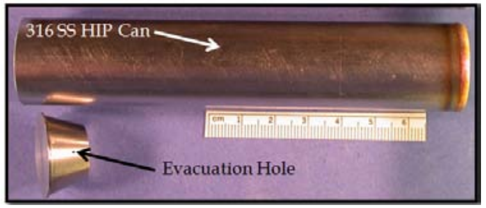


1) **Low temperature consolidation (700°C)**
   - Minimize oxygen exchange reaction
   - Study near-initial microstructure
2) **Heat treatment (1000°C and 1300°C)**
   - Explore the effects of Ti and Hf
   - Characterize microstructure evolution

THE Ames Laboratory
Creating Materials & Energy Solutions
U.S. DEPARTMENT OF ENERGY
U.S. DEPARTMENT OF ENERGY

Iowa State University of Science and Technology

# *As-Atomized Powder*

Fe-15.84Cr-0.50Ti-0.20Y-1.67O at.%
Fe-16.16Cr-0.94W-0.27Hf-0.08Y-0.23O at.%

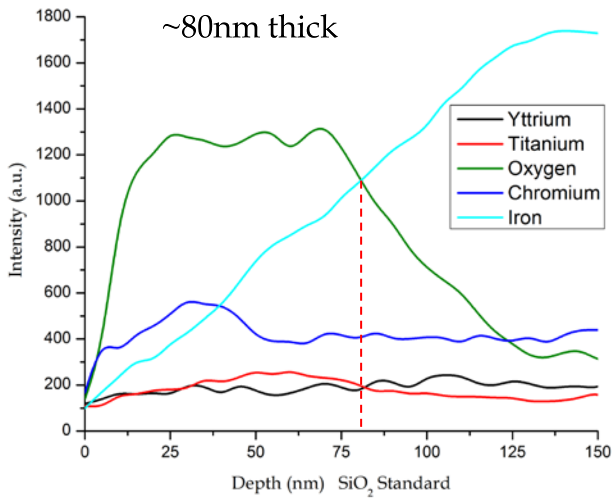


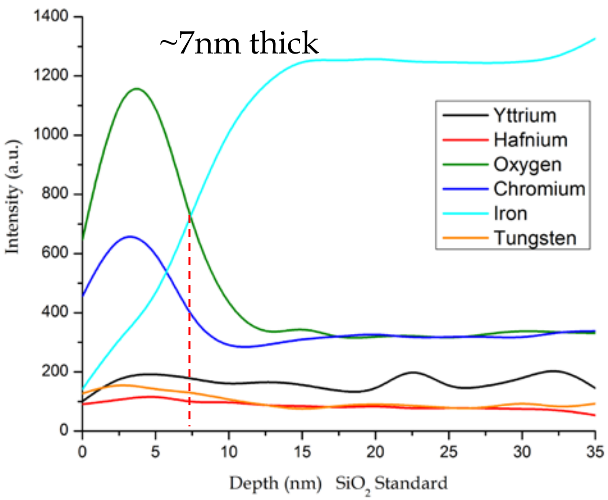


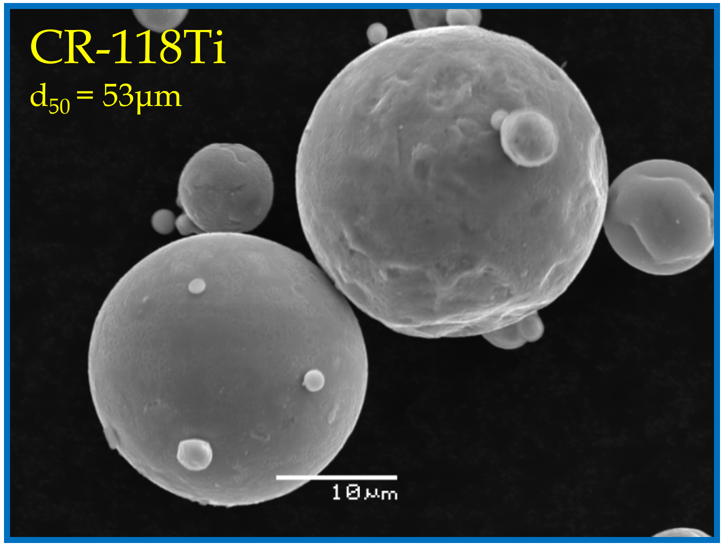


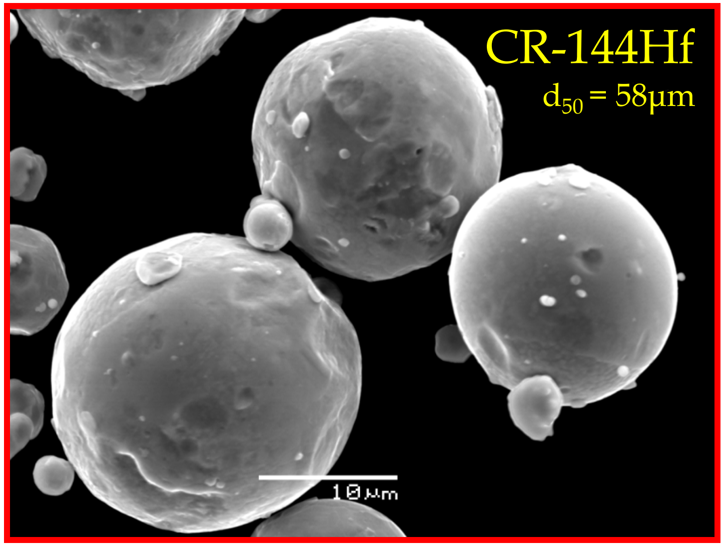

# As-Atomized Powder

**Fe-15.84Cr-0.50Ti-0.20Y-1.67O at.%**

**Fe-16.16Cr-0.94W-0.27Hf-0.08Y-0.23O at.%**

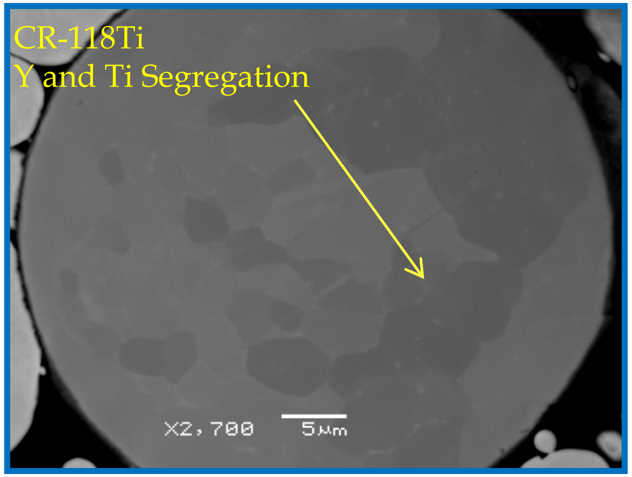


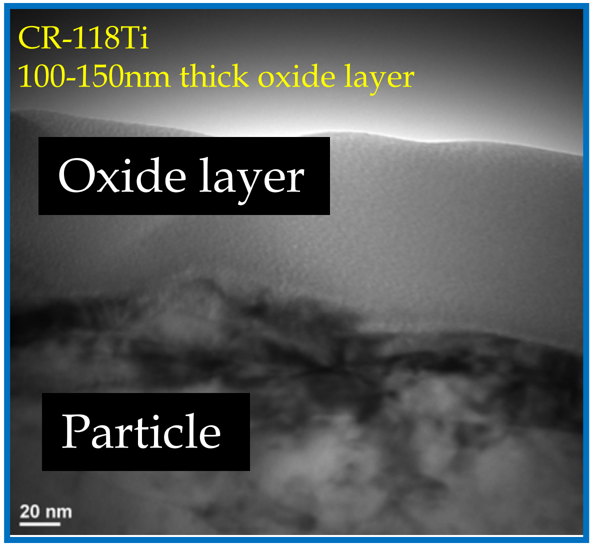


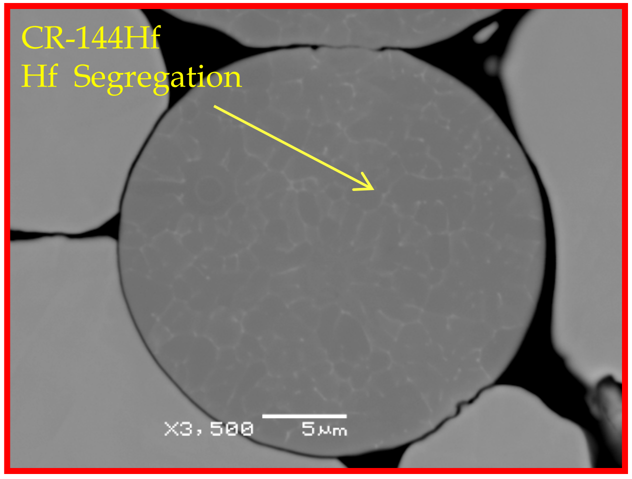


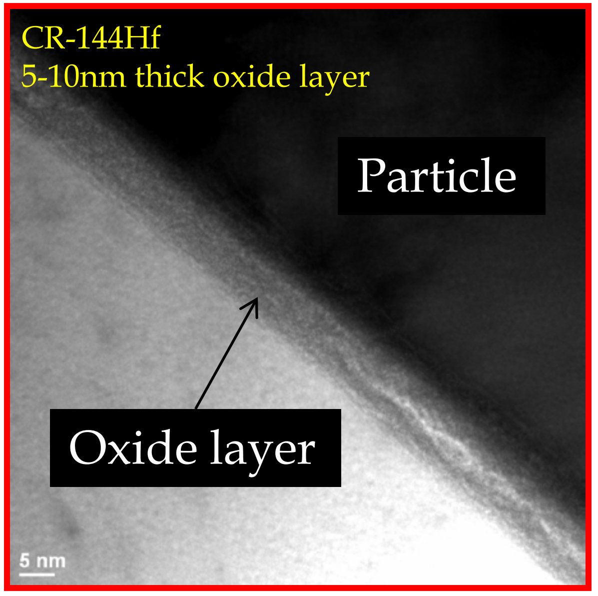

# As-HIPped (700 ℃) Microstructure

Fe-15.84Cr-0.50Ti-0.20Y-1.67O at.%
Fe-16.16Cr-0.94W-0.27Hf-0.08Y-0.23O at.%

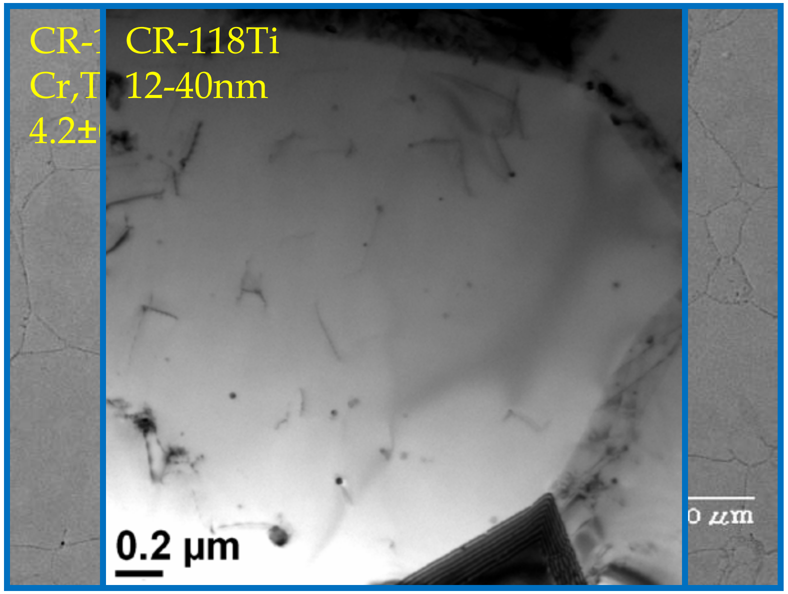


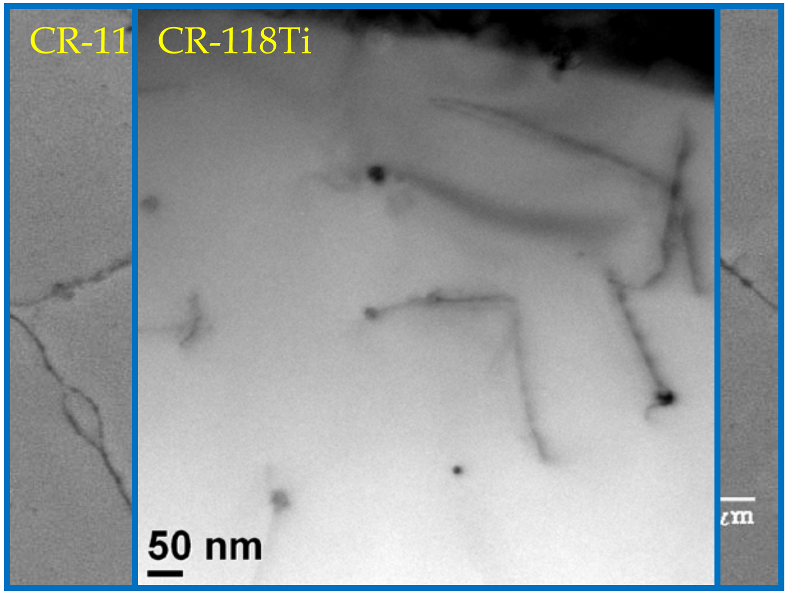


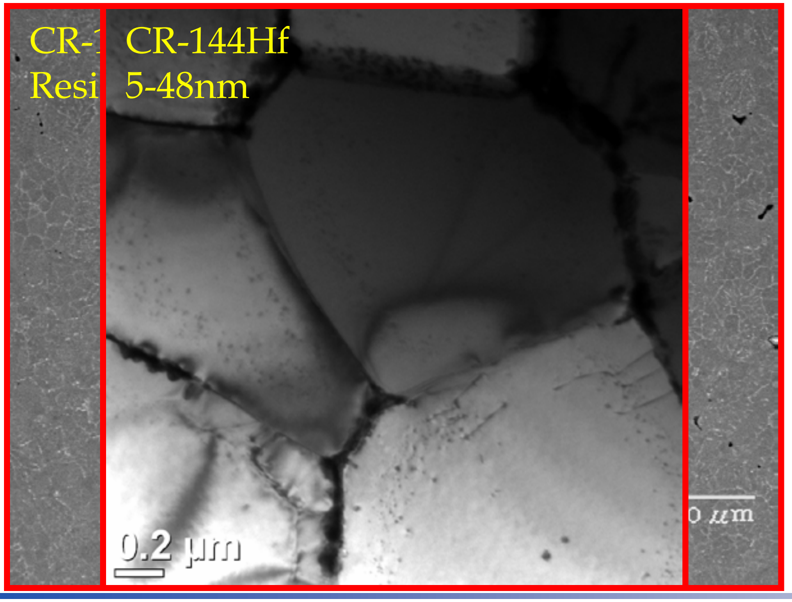


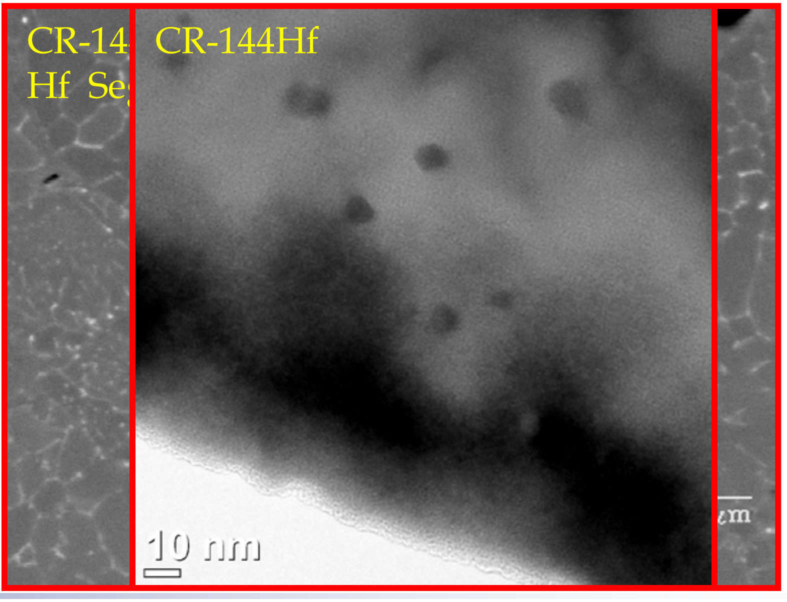

# *Heat Treated 1000 ℃-10hr-Vac.*

Fe-15.84Cr-0.50Ti-0.20Y-1.67O at.%

Fe-16.16Cr-0.94W-0.27Hf-0.08Y-0.23O at.%

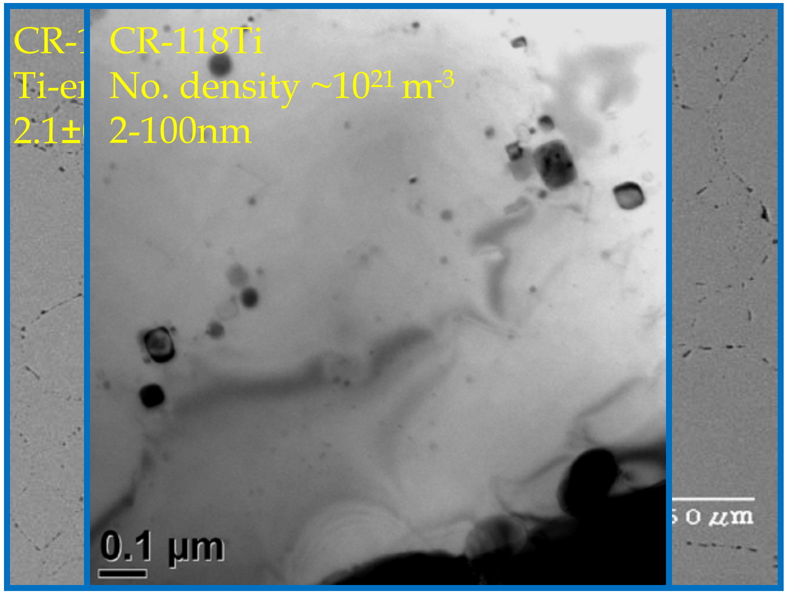


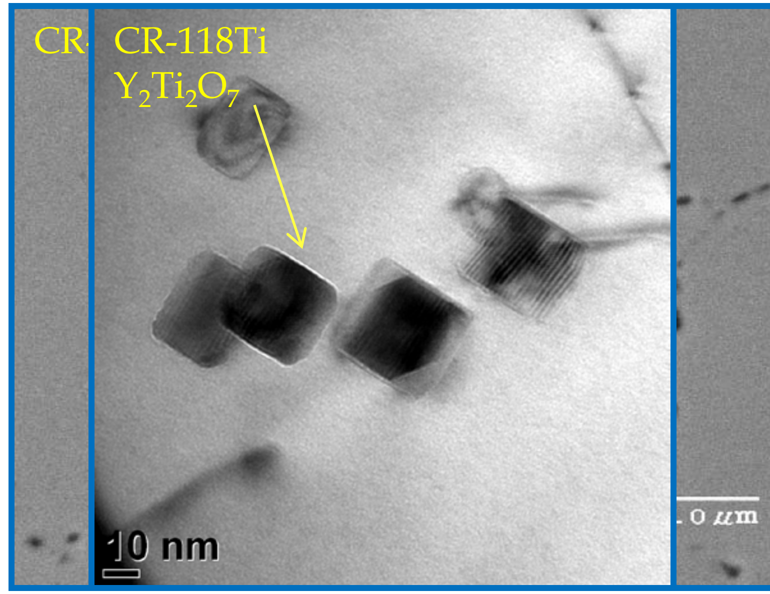


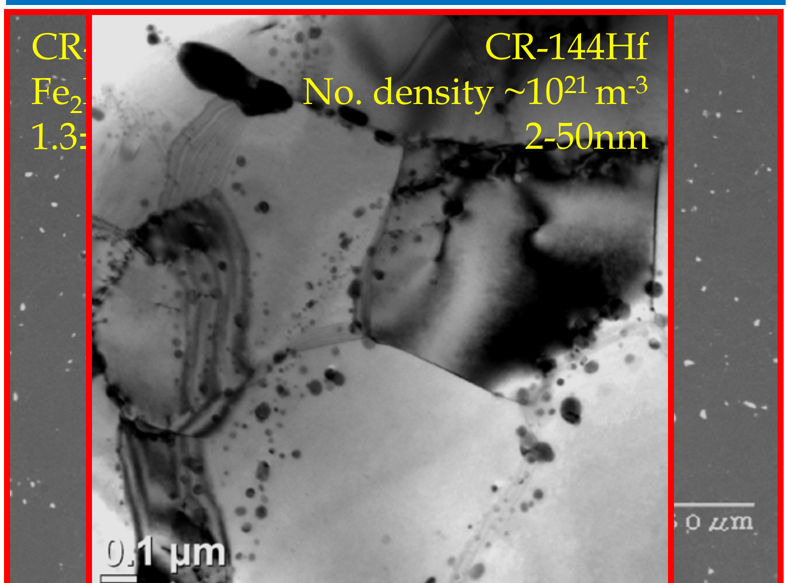


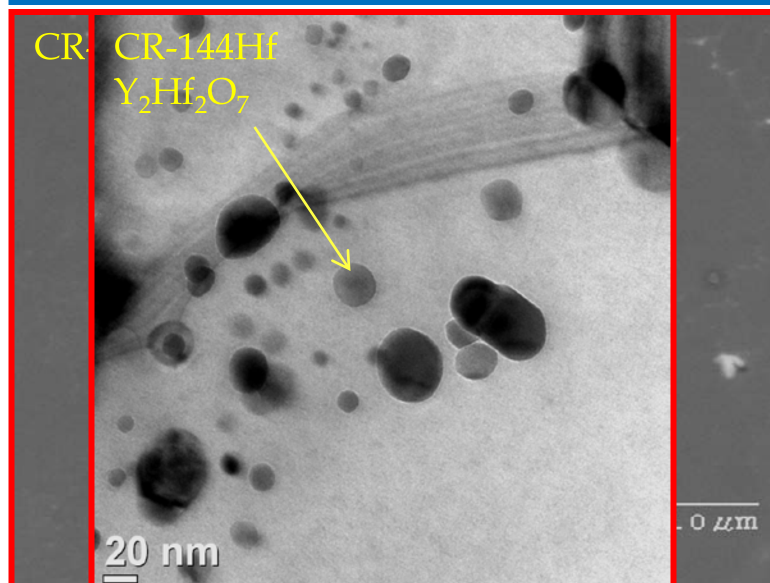


S. Ukai and S. Ohtsuka. Energy Materials, 2007. **2**(1): p. 26-35.

# *Heat Treated 1300 ℃-1hr-Vac.*

Fe-15.84Cr-0.50Ti-0.20Y-1.67O at.%
Fe-16.16Cr-0.94W-0.27Hf-0.08Y-0.23O at.%

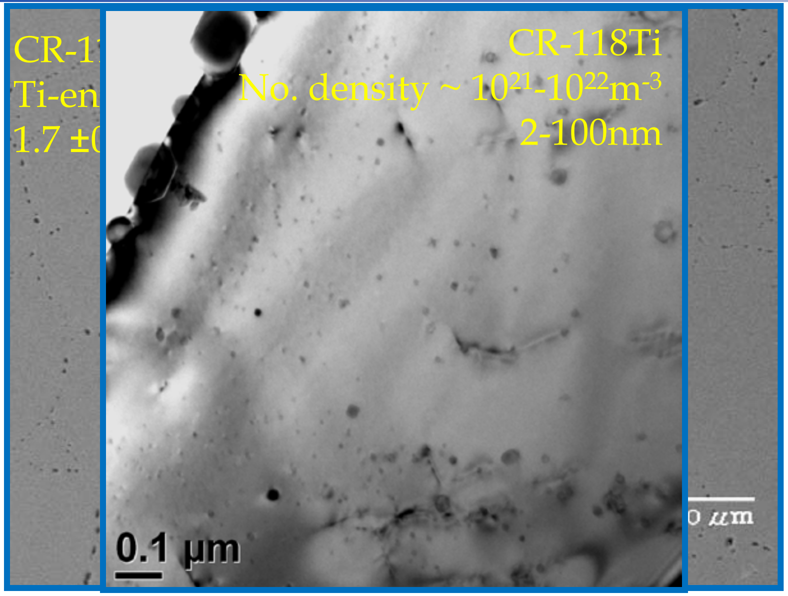


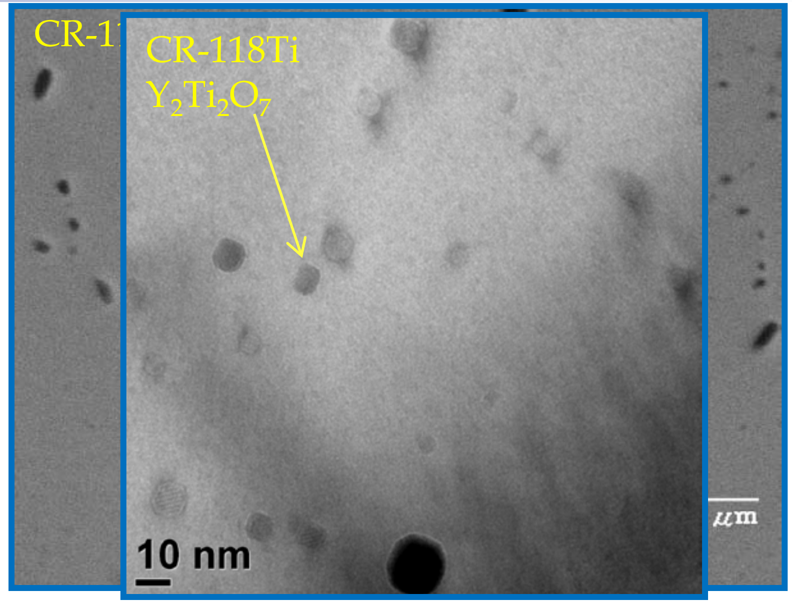


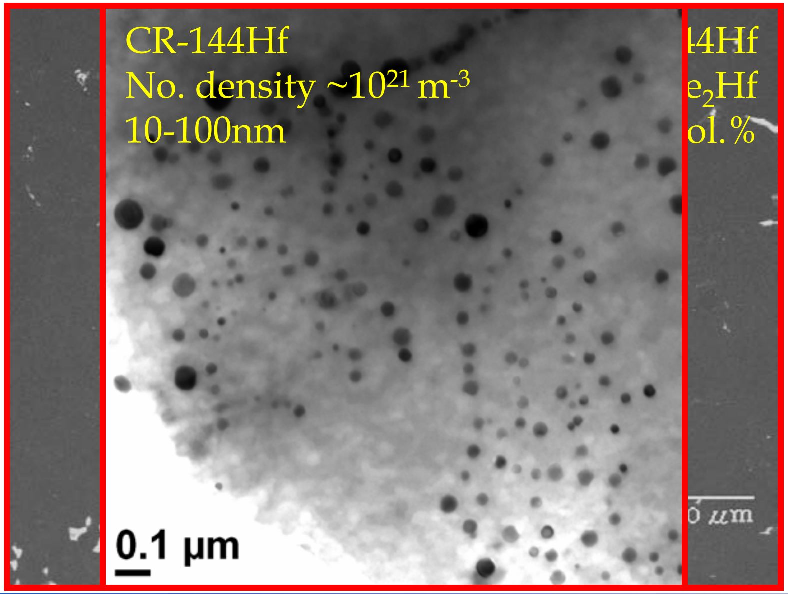


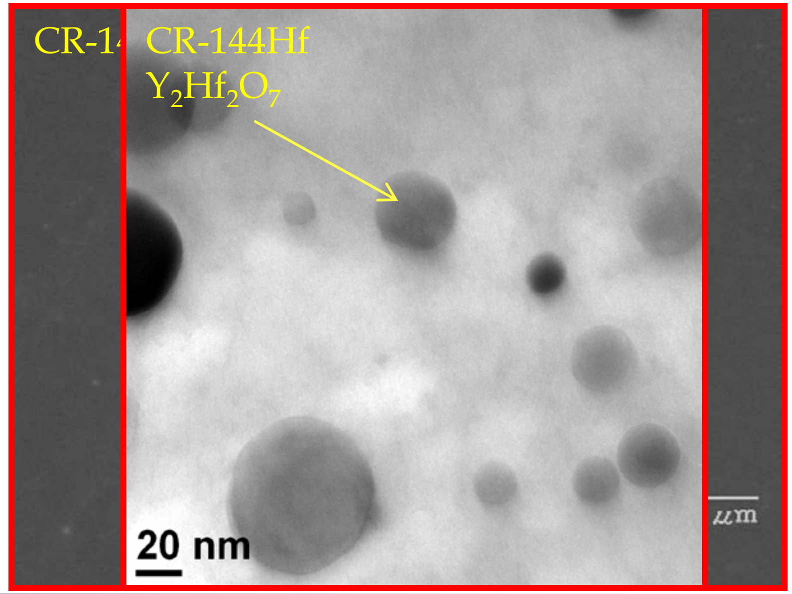

# Microstructure Evolution (CR-118Ti)

Fe-15.84Cr-0.50Ti-0.20Y-1.67O at.%
Fe-16.16Cr-0.94W-0.27Hf-0.08Y-0.23O at.%

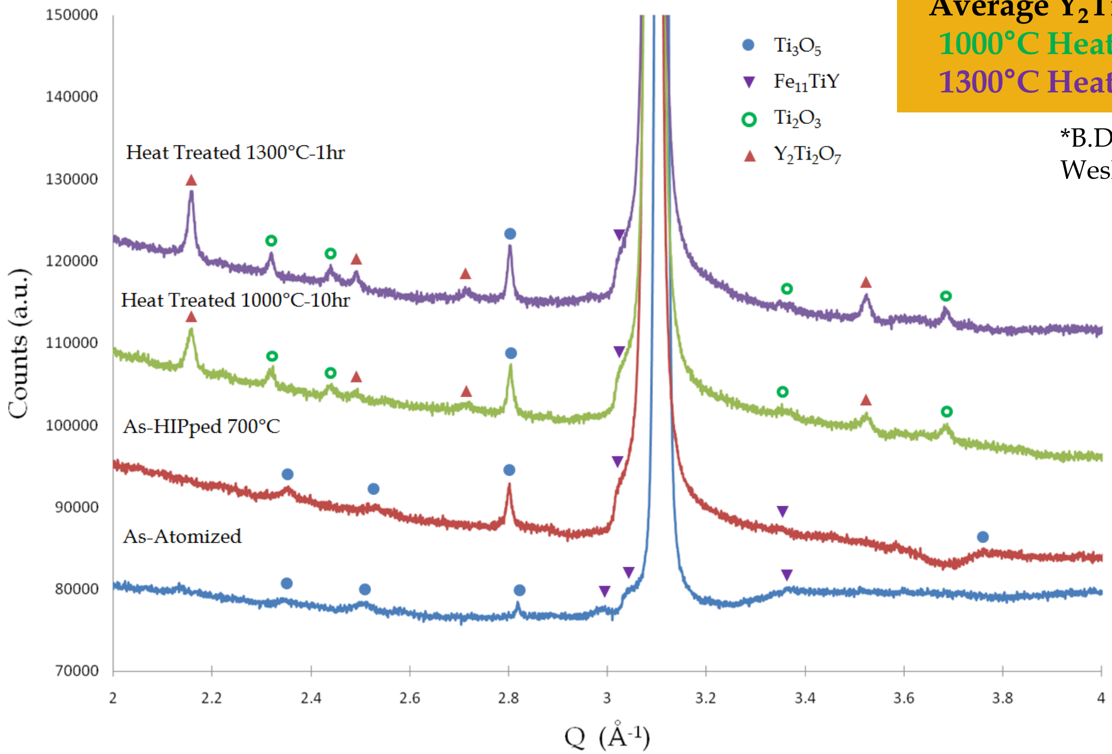


| Particle Size Analysis | *Scherrer Formula |
| --- | --- |
| Average $Y_2Ti_2O_7$ Crystallite size<br>1000°C Heat Treatment ~38nm<br>1300°C Heat Treatment ~45nm | $t \approx \frac{k\lambda}{\beta \cos\theta_\beta}$ |

*B.D. Cullity, Elements of X-Ray Diffraction, Addison-Wesley Publishing Company, Inc., 1967, p 99.

## Oxide Stability

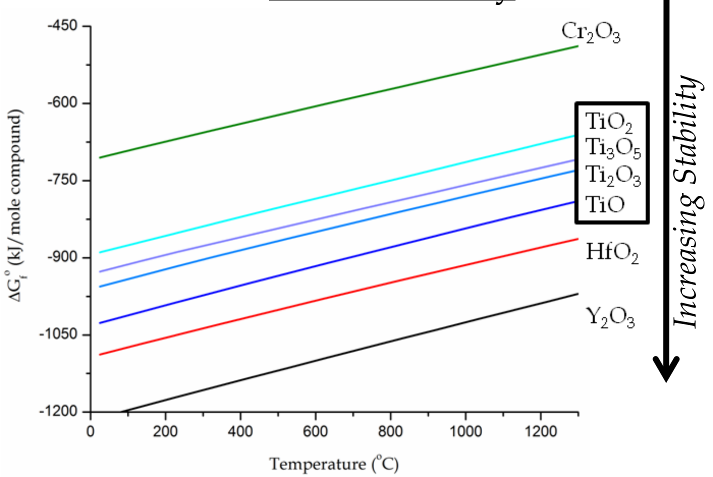


$$Cr_xO_{y\,(initial\ amorphous\ PPB\ oxide)} + Ti_{ss} \xrightarrow[consolidation]{700^oC} Ti_3O_5 + Cr_{ss}$$

$$Ti_3O_5 \xrightarrow[1000°C\ or\ 1300°C]{heat\ treatment} Ti_2O_3 + O_{ss}^{2-} \xrightarrow{Dispersoid\ Formation} Fe_{11}TiY + O_{ss}^{2-} \xrightarrow[internal\ oxidation]{**diffusionless} Y_2Ti_2O_7 + Fe_{ss}$$

**F. Gesmundo, and B. Gleeson, *Oxidation of Multicomponent Two-Phase Alloys.* Oxidation of Metals, 1995. **44**: p. 211-237.

# *Microstructure Evolution(CR-144Hf)*

$Fe$-15.84Cr-0.50Ti-0.20Y-1.67O at.%
$Fe$-16.16Cr-0.94W-0.27Hf-0.08Y-0.23O at.%

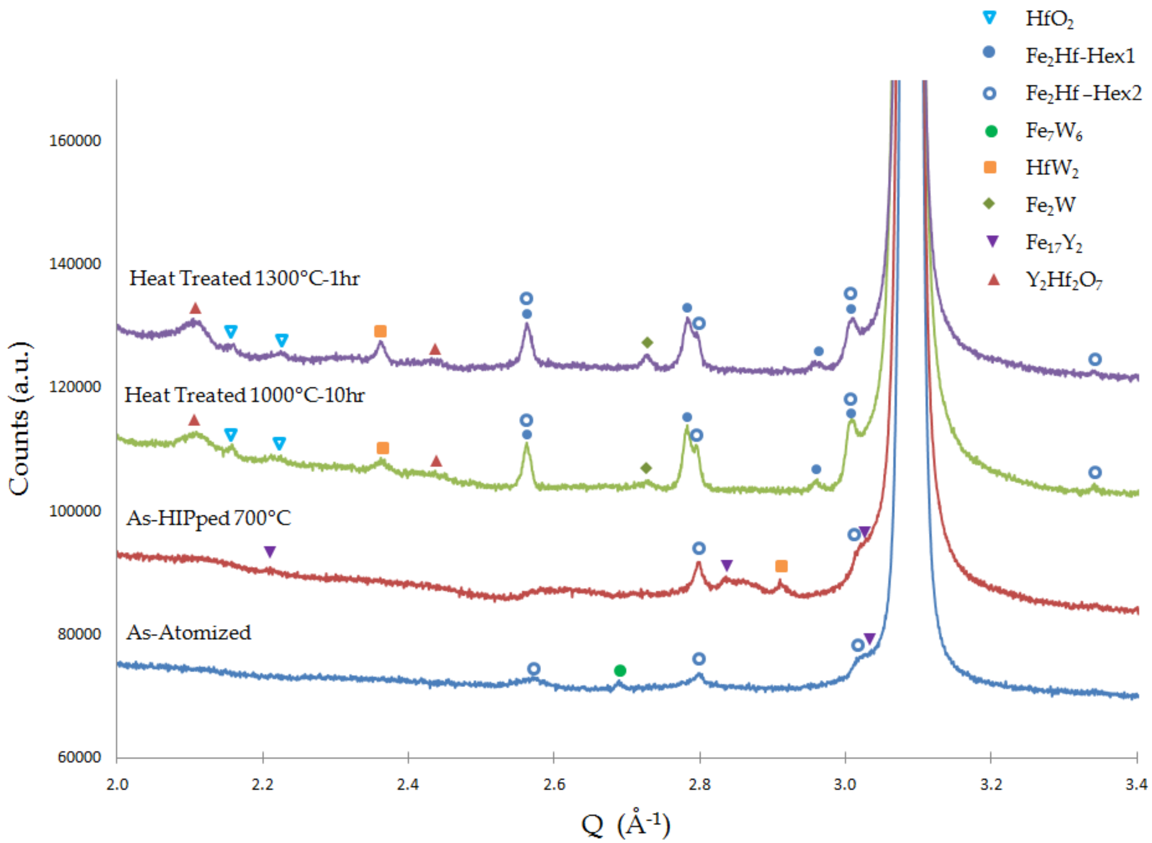


**Scherrer Particle Size Analysis**

**Average $Y_2Hf_2O_7$ Crystallite size**
**1000°C Heat Treatment ~10nm**
**1300°C Heat Treatment ~16nm**

- ❖ $Y_2Hf_2O_7$ dipsersoid formation during heat treatment (oxygen exchange reaction)
- ❖ Excess Hf content resulted in significant $Fe_2Hf$ intermetallic formation

$Fe_2Hf$-(Hex 2) —— $Y_2Hf_2O_7$ Dispersoid Formation ——→ $Fe_2Hf$-(Hex1) ($Fe_{2.3}Hf$-Hex 1)*

*Decreased Hf Content*




H. Okamoto, Iron-Hafnium Binary Diagram, ASM Handbook, vol.2, 1990.
ASM International Phase Diagram Center

# CR-Alloy Comparison

Fe-15.84Cr-0.50Ti-0.20Y-1.67O at.%
Fe-16.16Cr-0.94W-0.27Hf-0.08Y-0.23O at.%

| Alloy | ~Y (at.%) | ~O (at.%) | Experimental O/Y | Dispersoid | Ideal O/Y | Microstructure Defect |
|---|---|---|---|---|---|---|
| CR-118 | 0.2 | 1.67 | ~8.35 | $Y_2Ti_2O_7$ | 3.5 | Residual PPB oxide |
| CR-144 | 0.08 | 0.23 | ~2.88 | $Y_2Hf_2O_7$ | 3.5 | Residual $Fe_2Hf$ Precipitates |

- *Ideal microstructure* formation is directly related to achieving an *ideal O/Y* ratio in the initial precursor powders

- Careful control of dispersoid stabilizing elements (Ti, Hf) should help prevent the formation of unfavorable intermetallic phases ($Fe_2Hf$)

| Alloy | Dispersoid | Morphology | Avg. Size (nm) Apparent |
|---|---|---|---|
| CR-118Ti | $Y_2Ti_2O_7$ | Cuboidal | ~40-45 |
| CR-144Hf | $Y_2Hf_2O_7$ | Spherical | ~10-15 |



Y. Uchida, et al., Mater. Res. Soc. Symp. Proc., 2007. **981**: p. 09-14

# Diffusivity Comparison

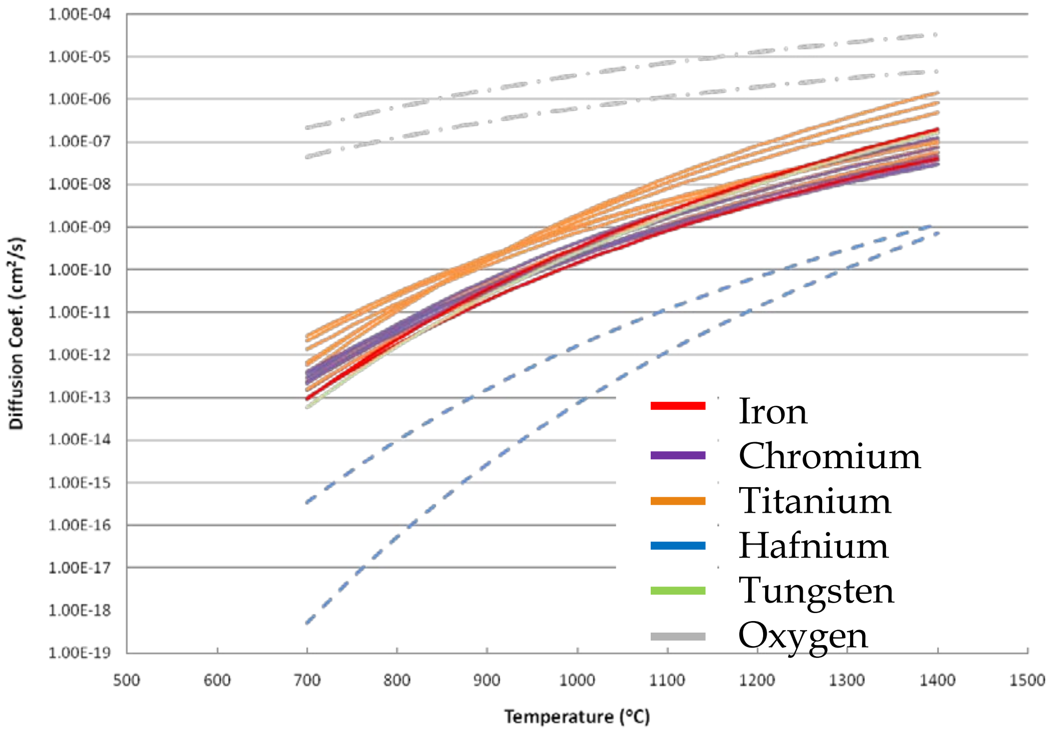


## Precipitate Growth

$$R = k(Dt)^{\frac{1}{2}}$$

$$k = -\frac{(C_I - C_M)}{2(C_P - C_I)}$$

D = volume diffusivity coefficient
$C_I$ = concentration at the precipitate/matrix interface
$C_M$ = concentration in the matrix at a remote point
$C_P$ = solute concentration in the precipitate

## Precipitate Coarsening (Ripening)

$$r^n = kt$$

r = precipitate radius
n = rate limiting exponent
k = material constant (diffusion mechanism and temperature)
t = coarsening time

| Exponent (n) | Rate Limiting Step |
|---|---|
| **2** | Atom transfer across interface |
| **3** | Matrix diffusion |
| **4** | Grain boundary diffusion |
| **5** | Dislocation pipe diffusion |

The slower diffusion kinetics of Hf compared to Ti in α-Fe could be the reason for smaller precipitate formation in CR-144

# CR-Alloy Microstructure Summary

- A new simplified processing* technique involving gas atomization and in situ oxidation has been developed to produce precursor ferritic stainless steel powder that can be consolidated into an oxide dispersion strengthened alloy with an isotropic microstructure
- Oxygen content in the powders is directly linked to the atomization processing parameters (Ar-$O_2$ vol.% and reaction temperature)
- **Results have shown a clear ability to manipulate the phase microstructure using elevated temperature heat treatment**
- Phase analysis confirms formation of nano-metric Y-enriched oxide dispersoids during elevated temperature heat treatments in both CR-118Ti and CR-144Hf
- Reduced average oxide dispersoid size may be possible utilizing Hf alloying additions ($Y_2Hf_2O_7$)
- Further characterization will be necessary in determining preferred dispersoid stabilizing element (Ti or Hf)



*I.E. Anderson, and (estate of) R.L. Terpstra, "Dispersoid Reinforced Alloy Powder and Method of Making," USPTO No. 7,699,905 B1, April 20th, 2010.

# *Internal Oxidation (Experimental Results)*

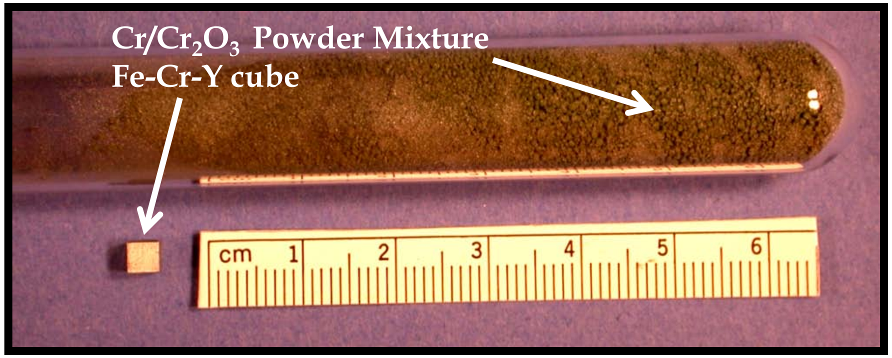


| Temperature (°C) | Time (hrs) |
|---|---|
| 1000 | 12, 72, 120 |
| 1100 | 4, 12, 24 |
| 1200 | 1, 2, 3 |
| 1300 | 1, 2, 3 |

- "Diffusionless" internal oxidation
- Chill Cast: Fe-15Cr-2Y (wt.%)
- $Cr/Cr_2O_3$ Rhines Pack
- $O_2$ Partial Pressure Control (Buffer)
- Prevents Exterior Scale Formation

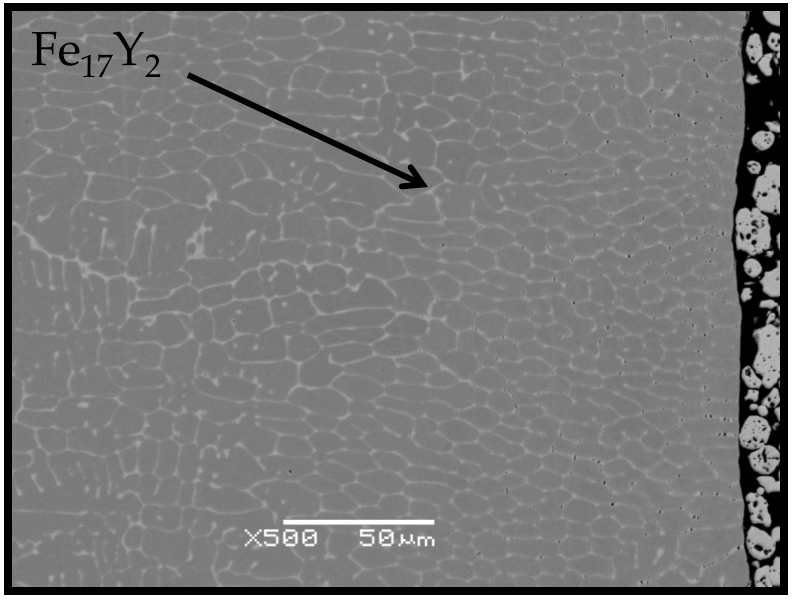


F. Gesmundo, and B. Gleeson, Oxidation of Metals, 1995. **44**: p. 211-237

# *Internal Oxidation Mechanism*

- Diffusionless or *"in situ"* internal oxidation
- Restricted metal diffusion (located at cell boundaries)
- Reservoirs (at prior particle boundaries) supply oxygen
- Assumes bulk diffusion

F. Gesmundo, and B. Gleeson, Oxidation of Metals, 1995. **44**: p. 211-237

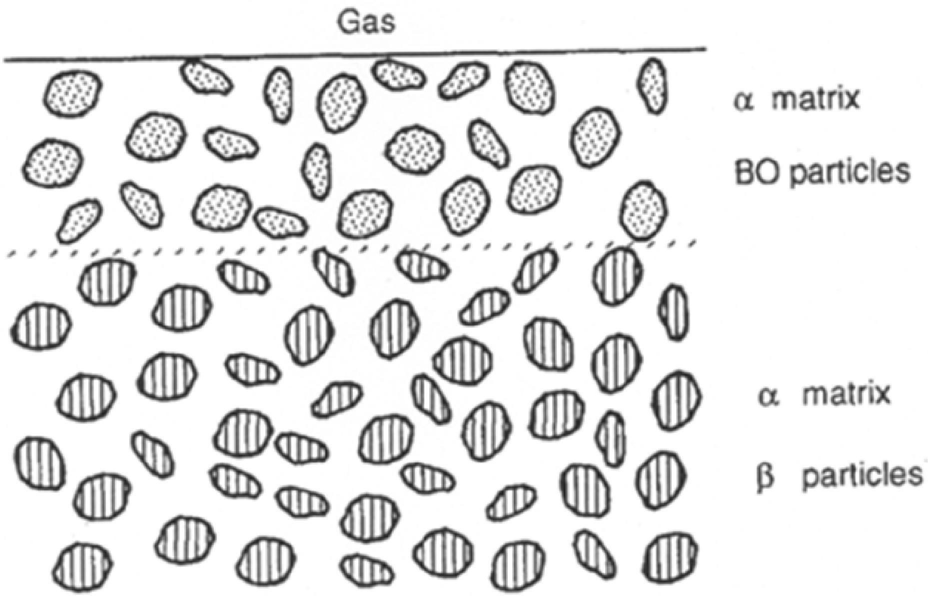


$$D_O = \frac{\xi^2}{4\gamma^2 t}$$

$$\frac{N_O^s}{N_Y^o} = \frac{\nu G(\gamma)}{F(h)} \rightarrow \frac{N_O^s}{N_Y^o} = \nu G(\gamma)$$

C. Wagner, Elektrochemie, 1959. **63**: p. 772-782
R. A. Rapp, Corrosion, 1965. **21**: p. 382-389.

$$G(\gamma) = \pi^{\frac{1}{2}} \gamma \exp(\gamma^2) \frac{2}{\pi^{\frac{1}{2}}} \int_0^{\gamma} \exp(-y^2) dy \quad F(h) = \pi^{\frac{1}{2}} h \exp(h^2) \frac{2}{\pi^{\frac{1}{2}}} \int_0^{h} \exp(-y^2) dy \quad h = \gamma \left(\frac{D_O}{D_Y}\right)^{\frac{1}{2}}$$

# Internal Oxidation (Experimental Results at 1100˚C)

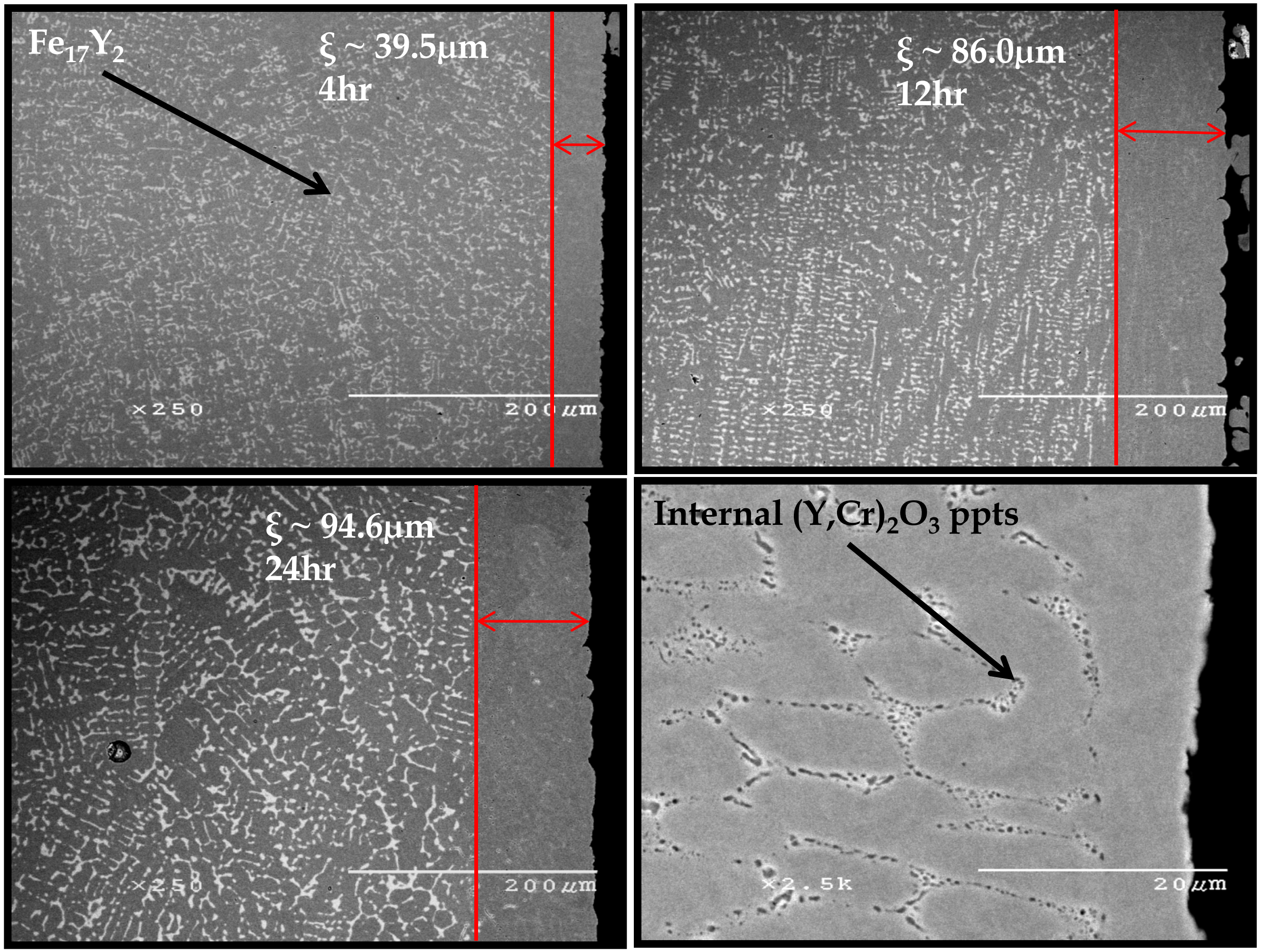


➢ Internal oxidation controlled by diffusion, IMC transformed to oxide particles.

# *Internal Oxidation Kinetics*

$$D_O = \frac{\xi^2}{4\gamma^2 t}$$

$$\frac{N_O^s}{N_Y^o} = \nu G(\gamma)$$

$$N_O^S \approx K_{O_2}\left(P_{O_2}{}^{\frac{1}{2}}\right)$$

C. Wagner, Elektrochemie, 1959. **63**: p. 772-782
R. A. Rapp, Corrosion, 1965. **21**: p. 382-389.

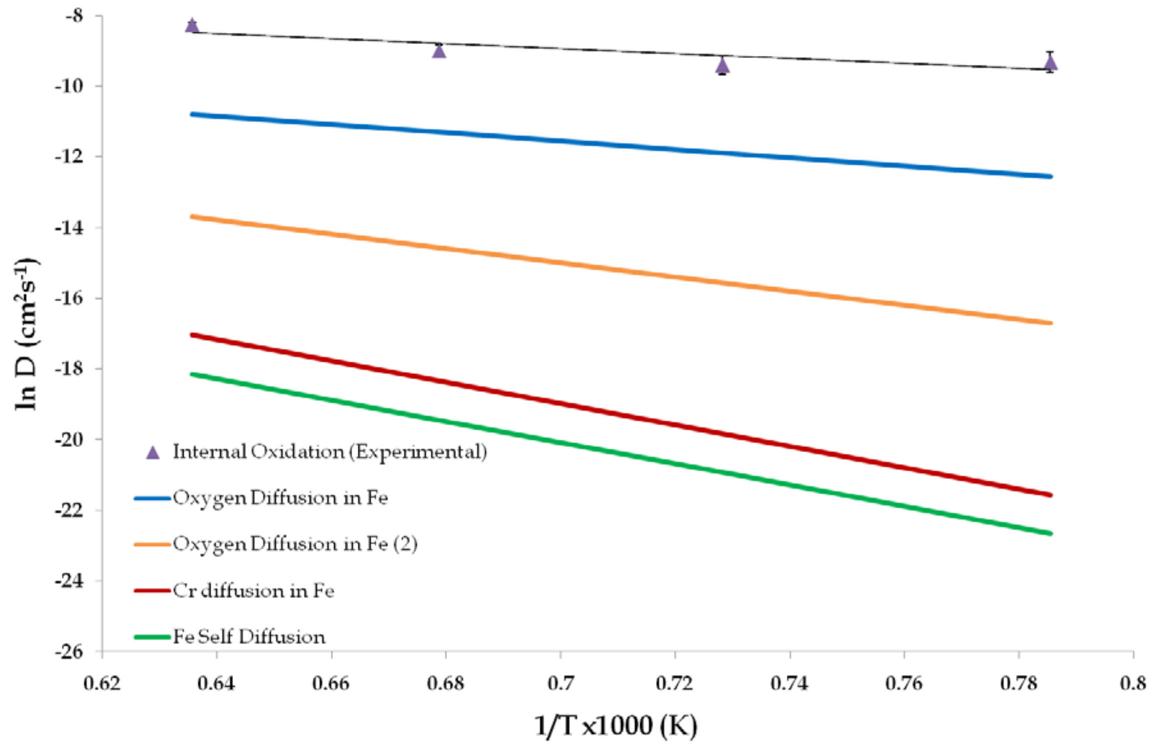


- Sievert's Law (oxygen solubility)
- Experimental oxygen diffusion coefficient
- Possible increased diffusion along phase boundaries

| Diffusion Species | Q (kJ) | A ($cm^2s^{-1}$) |
|---|---|---|
| O in Fe (experimental) | ~57.5 | ~0.017 |
| O in Fe | 98.0 | 0.037 |
| O in Fe | 167.1 | 0.4 |
| Cr diffusion in Fe | 250.8 | 8.52 |
| Fe self diffusion in Fe | 258.3 | 6.8 |



D.J. Young, *High Temperature Oxidation and Corrosion of Metals*. Vol. Vol. 1. 2008: Elsevier Science. 592

# Heat Treatment Predictions

Newest Alloy!!

| Alloy | Fe (at.%) | Cr (at.%) | W (at.%) | Ti (at.%) | Hf (at.%) | Y (at.%) | O (at.%) | Rxn Gas (vol.%) | Rxn Gas Inlet |
|---|---|---|---|---|---|---|---|---|---|
| CR-156 | 84.49 | 15.84 | - | - | 0.11 | 0.18 | 0.38 | Ar-0.12$O_2$ | HPGA Nozzle |

| Temperature (°C) | $\gamma^2$ | $D_O$ ($cm^2s^{-1}$) | k ($cm^2s^{-1}$) |
|---|---|---|---|
| 1000 | 2.87302E-06 | 3.66596E-06 | 4.21294E-11 |
| 1100 | 1.13492E-05 | 7.17649E-06 | 3.2579E-10 |
| 1200 | 3.70635E-05 | 1.28242E-05 | 1.90124E-09 |
| 1300 | 0.000103175 | 2.67893E-05 | 8.78475E-09 |

| Temperature (°C) | H.T. Time (hr) |
|---|---|
| 1000 | 23.2 |
| 1100 | 3.00 |
| 1200 | 0.51 |
| 1300 | 0.11 |

$$k_{ox} = 4\gamma^2 D_O \qquad t = \frac{x^2}{2k_{ox}}$$

- Reaction time required for internal oxidation from PPB to particle core
- Model will need to be tested on future CR-alloys to confirm mechanism
- Prevent unnecessary dispersoid growth or coarsening

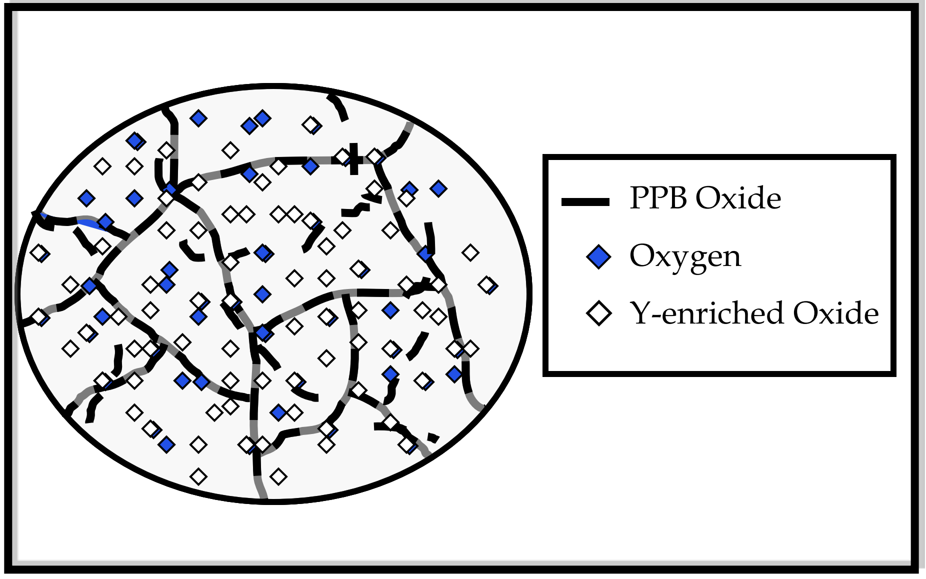

# *Future Work*

**FY2010**

- **Modify the GARS processing parameters (reaction gas content) to move closer to an ideal Y/O ratio in the precursor oxide dispersion forming ultrafine powders.**
  - **Fe-Cr-Hf-Y (Ar-0.1$O_2$ vol.%)**
  - **Fe-Cr-Ti-Y (Ar-0.1$O_2$ vol.%)**

- **Utilize results of high temperature studies of the transformation kinetics of consolidated CR-alloys to select heat treatment parameters and initiate mechanical deformation studies for producing high performance ODS alloys.**

**FY2011**

- Continue analysis of different dispersoid stabilizing elements (Ti and Hf)
  - TEM/EFTEM
  - HE-XRD (Synchrotron)

- High Temperature Strength Analysis (Mechanical Properties)
  - Elevated temperature tensile and creep properties
  - Can these new CR-alloys meet the critical high temperature strength requirements?

*P. Miao, et al., Nuclear Materials, 2008. **377**: p. 59-64.

# *Reactive Atomization Process Control*

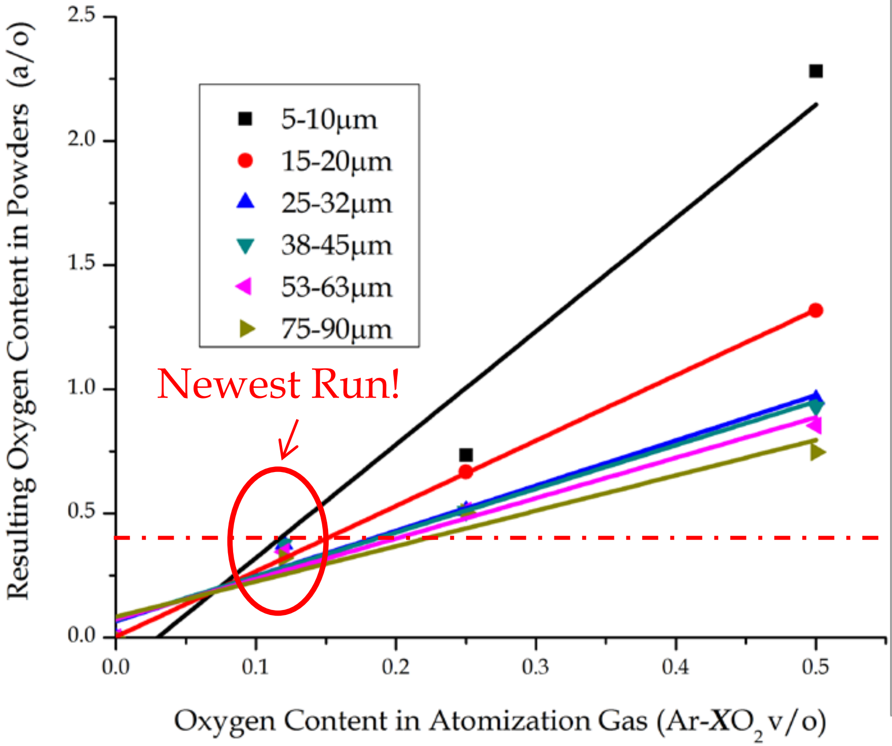


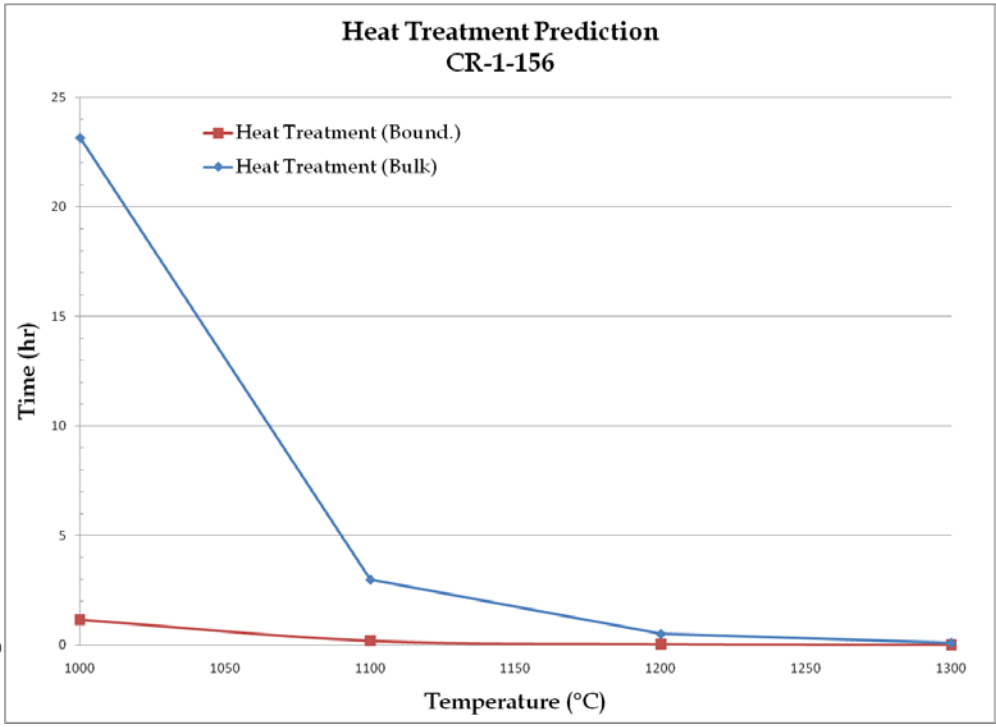


| | Alloy | Fe (at.%) | Cr (at.%) | Ti (at.%) | Hf (at.%) | Y (at.%) | O (at.%) | Rxn Gas (vol.%) | Rxn Gas Inlet |
|---|---|---|---|---|---|---|---|---|---|
| Alloy Design | CR-156Hf | Bal. | 15.94 | - | 0.12 | .124 | 0.414 | Ar-0.12$O_2$ | HPGA Nozzle |
| Resulting Composition | CR-156Hf | 84.49 | 15.84 | - | 0.11 | 0.18 | 0.38 | Ar-0.12$O_2$ | HPGA Nozzle |

# Dislocation Substructure Formation (TMT)

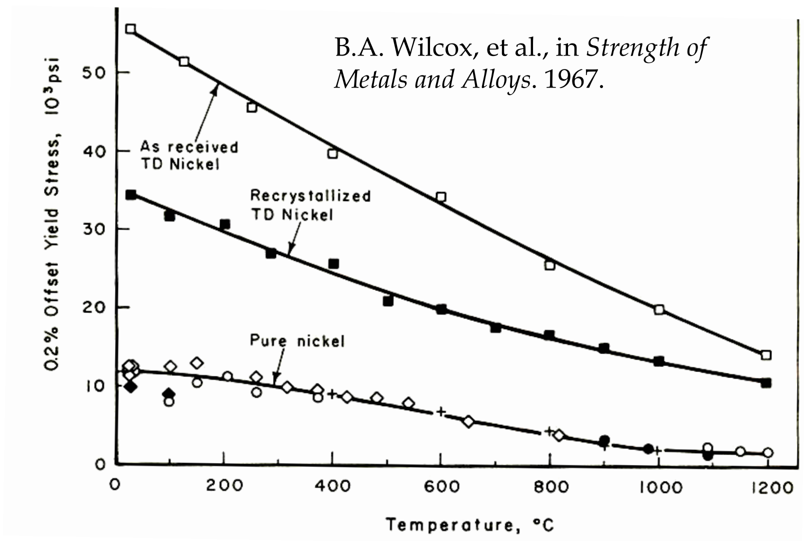


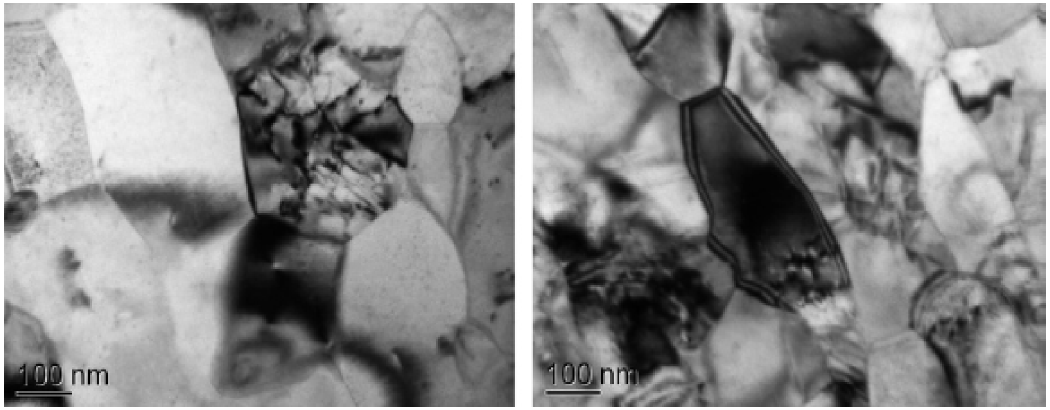


NFA 14YWT

P. Miao, et al., Nuclear Materials, 2008. **377**: p. 59-64

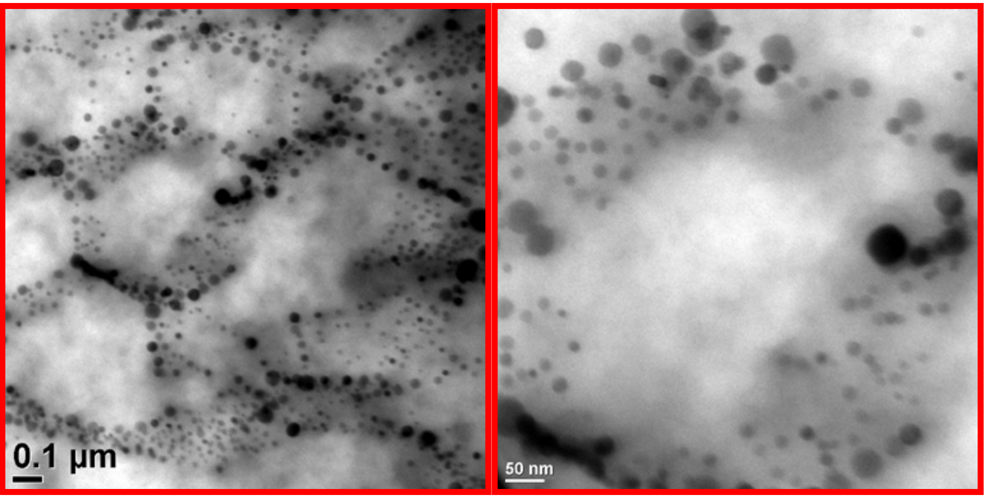


CR-144 (-20μm)
HT 1300°C-1hr

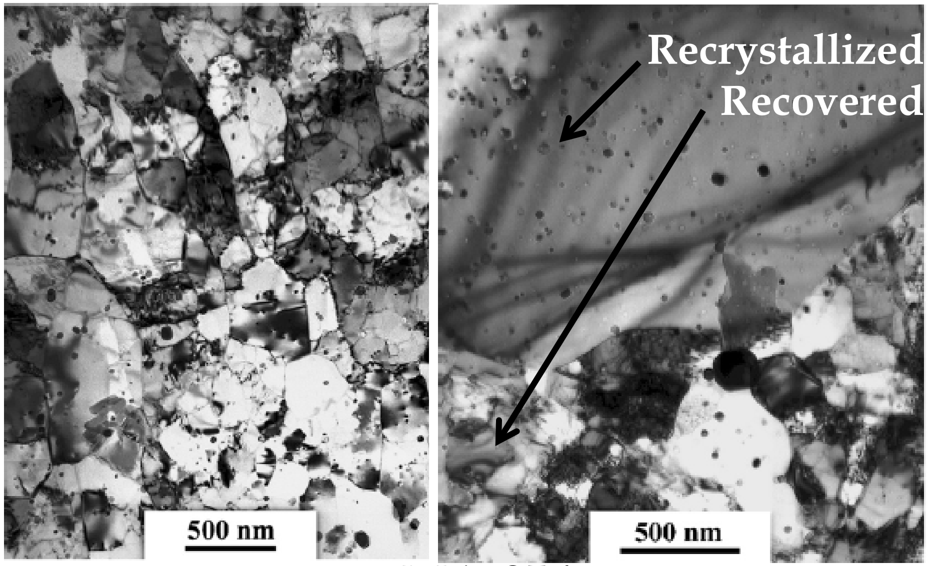


MA-956

M.F. Hupalo, et al., ISIJ International, 2004. **44**(11)

# *Acknowledgments*

❖ ***Support from the Department of Energy-Office of Fossil Energy is gratefully acknowledged through Ames Laboratory contract no. DE-AC02-07CH11358.***

***Dr. Danny Shechtman[1], Jim Anderegg[1], Hal Sailsbury[1], Matt Besser[1], Jamie Thompson[2], and Andrew Steinmetz[2]***

***1US Dept. of Energy Ames Laboratory,***
***Materials and Engineering Physics, Ames, IA 50011***

***2Iowa State University, Material Science and Engineering (Undergraduate Student), Ames, IA 50011***